Journal of Solid State Chemistry **156,** 470–479 (2001)
doi:10.1006/jssc.2000.9026, available online at http://www.idealibrary.com on IDEAL®

# Lithium-Ion Conductors of the System $LiCo_{1-x}Fe_xO_2$, Preparation and Structural Investigation

M. Holzapfel,[1] C. Haak, and A. Ott

*Institut für Anorganische Chemie, Universität Tübingen, Auf der Morgenstelle 18, 72070 Tübingen, Germany*

Received July 18, 2000; in revised form October 18, 2000; accepted November 6, 2000

DEDICATED TO PROFESSOR DR. SIBYLLE KEMMLER-SACK

**Layered structure oxides of the system $NaCo_{1-x}Fe_xO_2$ were prepared for $0 \leq x \leq 1$ by solid-state reaction. Vegard-like behavior was proved for these compounds by X-ray analysis, indicating mixed transition metal layers and sodium layers without cation disorder. By ion-exchange of these compounds in a molten eutectic mixture of LiCl and $LiNO_3$ at 260°C the system $LiCo_{1-x}Fe_xO_2$ was prepared for the whole composition range and characterized by chemical analysis, X-ray diffraction and FTIR spectroscopy. Atomic absorption spectroscopy showed almost complete ion-exchange from sodium to lithium. The members of this system are shown to crystallize, as the sodium compounds, in the rhombohedral space group $R\bar{3}m$ (α-$NaFeO_2$-type). X-ray diffraction, considerations based on the intensity ratio $R_{101} = I_{101}/I_{104}$ and Rietveld refinement give evidence for increasing cation disorder with increasing iron content, that reaches the value of $LiFeO_2$ (4.5%) already at an iron content of $x = 0.4$.**



***Key Words:*** **oxidic materials; layered structures; ion exchange reaction; lithium batteries; rechargeable.**

## 1. INTRODUCTION

Layered transition metal oxides with α-$NaFeO_2$-type structure have been thoroughly investigated because of their possible use as materials in 4-V rechargeable lithium ion batteries. The rhombohedral structure is made up of lithium and transition metal cations that occupy the octahedral sites of a cubic close packing of oxide ions. Li is present on the 3*a* sites, *M* on the 3*b* sites, and O on the 6*c* sites of the hexagonal structure with $R\bar{3}m$ space group.

$LiMO_2$ compounds of the first transition metal series crystallize in different structure types, depending on the size of the *M* cation. For $M$ = V, Cr, Co, and Ni the compounds adopt the layered rock salt structure, while for $M$ = Ti, Mn, and Fe other structure types are found.

$LiTiO_2$ shows disordered rock salt structure (1). $LiMnO_2$ obtained by solid-state reaction crystallizes in an orthorhombic corrugated layer structure (2, 3), which transforms more or less rapidly to the spinel type structure on electrochemical cycling. Recently, $LiMnO_2$ with a layered rock salt structure was prepared either from α-$NaMnO_2$ by ion exchange reaction (4, 5) or directly by a hydrothermal method (6). $LiFeO_2$ exists in a variety of modifications, as cubic disordered rock salt structure α-$LiFeO_2$, monoclinic ordered rock salt type β-$LiFeO_2$, and γ-$LiFeO_2$ that crystallizes in a rhombohedral ordered rock salt structure (7, 8). None of these modifications shows electrochemical activity except for two recently discovered $LiFeO_2$-polymorphs: an orthorhombic corrugated layered structure (9–11) and an orthorhombic Goethite-type structure (11). $LiFeO_2$ with α-$NaFeO_2$-type structure which can be obtained from α-$NaFeO_2$ by ion exchange reaction (12–19), is not electrochemically active up to 4.5 V vs $Li/Li^+$. Possible explanations that have been considered to account for this fact are important $Fe^{3+}$ disorder in the 3*a* sites hindering the diffusion of the lithium ions, rapid structure change to disordered rock salt type α-$LiFeO_2$, and instability of the formed $Fe^{4+}$ ions (13, 20).

Stoichiometric $LiNiO_2$, the lithium-rich end member of the system $Li_{1-x}Ni_{1+x}O_2$, is difficult to prepare and always contains a small fraction of divalent nickel ions in the lithium layer (21, 22), increasing the three-dimensional character of the material which results in pure cubic rock salt phase, NiO, for $(1 - x) = 0$. For $LiCoO_2$ (23, 24) perfect structural ordering has been evidenced. Several attempts have been made to stabilize the layered structure of $LiNiO_2$ by substituting Co partially for Ni (25–29). The so obtained oxides are more easily prepared than $LiNiO_2$ and electrochemically more stable. Substituting iron in $LiFeO_2$ partially for cobalt can be thought to have an effect comparable to $LiNi_{1-x}Co_xO_2$, i.e., reducing the amount of $Fe^{3+}$ present

[1] To whom correspondence should be addressed at Laboratoire d'Electrochimie et de Physicochimie des Matériaux et des Interfaces (LEPMI), ENSEEG-INPG, 1130, rue de la piscine, BP 75, 38402 St. Martin d'Hères, France. Fax: + 33 (0)4 76 82 66 70. E-mail: michael.holzapfel@lepmi.inpg.fr.



0022-4596/01 $35.00

in 3*a* sites, thus facilitating lithium diffusion and perhaps rendering possible lithium deintercalation.

Nontoxicity and low cost of iron would make $LiCo_{1-x}Fe_xO_2$ an interesting cathode material for rechargeable lithium batteries. So far substitution of cobalt for iron has been investigated in the system $LiCo_{1-x}Fe_xO_2$ up to an iron content of $x = 0.3$ by solid-state, high-temperature synthesis (30, 31) but to our knowledge, no results have been published yet about the successfull synthesis of the system $LiCo_{1-x}Fe_xO_2$ over the whole composition range $0 \leq x \leq 1$.

In this work we present the results on the synthesis of the system $LiCo_{1-x}Fe_xO_2$ ($0 \leq x \leq 1$) obtained by ion exchange reaction from the corresponding $NaCo_{1-x}Fe_xO_2$ system ($0 \leq x \leq 1$) and its investigation by XRD, FTIR, and chemical analyses. Examinations by magnetic susceptibility measurements are published in (32), results of the electrochemical characterization will follow in (33).

## 2. EXPERIMENTAL

For the synthesis of members of the series $NaCo_{1-x}Fe_xO_2$ the starting materials $Na_2O_2$-powder (95%, Fluka), $Co_3O_4$ (puriss. p. A., Merck), and $Fe_2O_3$ (carbonyl iron oxide, BASF) were thoroughly mixed with 5% excess of $Na_2O_2$ (to account for volatilization losses) in an agate mortar in argon atmosphere (glove box MB 150 B-G, $O_2$ and $H_2O$ $< 1$ ppm). The powders were heated in air in corundum boats (Degussit Al 23) with intermittent grinding and X-ray analysis (Philips Powder Diffractometer PW1130/00, Ni-filtered Cu$K_\alpha$ radiation, Au-Standard).

Because of the moisture sensitivity of $NaCoO_2$ the cobalt-rich products were put into the glove box after firing.

The $LiCo_{1-x}Fe_xO_2$ compounds were obtained by reacting the $NaCo_{1-x}Fe_xO_2$ samples in an eutectic LiCl/$LiNO_3$ mixture (11.8 mol% LiCl, 88.2 mol% $LiNO_3$, FP: 253°C) at 253–260°C for 6 h. The molar ratio Na compound vs lithium salt was chosen 1:10.

The reaction products were washed with methanol (reinst, $> 99.5\%$, Merck), dried *in vacuo* at room temperature, and reacted a second time in the same manner.

The ion exchange reactions were carried out in air except for the cobalt rich phases ($0.7 \leq (1 - x) \leq 1$) which were reacted in argon because of the moisture sensitivity of $NaCoO_2$.

$LiCoO_2$ was also prepared using a conventional high temperature synthesis by firing a stoichiometric mixture of $Li_2CO_3$ (99.5%, Alfa) and $Co_3O_4$ in air at 900°C for 72 h. The product is further denoted HT-$LiCoO_2$ to distinguish it from the product obtained by ion exchange reaction, which is denoted IE-$LiCoO_2$.

The obtained reaction products were characterized by X-ray diffraction. Profile refinements were accomplished by Rietveld analysis using the program FULLPROF 90 (34) based on diffraction patterns obtained on a Philips PW1830 for diffraction angles $15° \leq 2\theta \leq 90°$. Chemical analyses were carried out using an atomic absorption spectrometer (Perkin-Elmer, Model 400) for the determination of the amounts of Li, Na, Co, and Fe present and a Metrohm 686 Titroprozessor for the determination of the average oxidation state of the transition metals.

## 3. RESULTS AND DISCUSSION

### 3.1. The System $NaCo_{1-x}Fe_xO_2$

Reaction temperature and firing times are listed in Table 1. The products were obtained as reddish-brown to black (with rising cobalt content) powders. For the preparation of α-$NaFeO_2$ (14, 15, 18, 35, 36) complete conversion was observed already after 12 h. For the synthesis of the phases with low cobalt content, $(1 - x) = 0.1$–$0.2$, the reaction temperature had to be risen for more than 200°C to complete the reaction. The trend to higher temperatures and longer firing periods is continued until $(1 - x) = 0.6$. At $(1 - x) = 0.7$ a sudden change takes place: the reaction temperature still being high, the reaction period had to be reduced drastically and the products had to be quenched to room temperature. Otherwise, the formation of a second phase took place on cooling, resembling to monoclinic α′-$NaCoO_2$ (37, 38) (or monoclinic α′-$NaCoO_2$ itself while a third, iron-rich phase that should also be formed to compensate for the iron deficiency could not be detected by XRD). For $(1 - x) = 0.9$ the formation of the second phase was much slower and for $NaCoO_2$ the reaction temperature had to be lowered drastically to avoid the formation of monoclinic α′-$NaCoO_2$ (which is known to occur at 750°C (38)) as much as possible.

According to the XRD-results (Fig. 1) the products were obtained single phase crystallizing in the rhombohedral

**TABLE 1**
**Reaction Conditions for the Preparation of the $NaCo_{1-x}Fe_xO_2$ Compounds**

| Stoichiometry | Reaction temperature (°C) | Reaction periods (h) | Remarks |
|---|---|---|---|
| $NaFeO_2$ | 500 | 12 | |
| $NaCo_{0.1}Fe_{0.9}O_2$ | 750 | 48 | |
| $NaCo_{0.2}Fe_{0.8}O_2$ | 750 | 120 | |
| $NaCo_{0.3}Fe_{0.7}O_2$ | 800 | 120 | |
| $NaCo_{0.4}Fe_{0.6}O_2$ | 900 | 96 | |
| $NaCo_{0.5}Fe_{0.5}O_2$ | 850 | 96 | |
| $NaCo_{0.6}Fe_{0.4}O_2$ | 900 | 96 | |
| $NaCo_{0.7}Fe_{0.3}O_2$ | 900 | 3 | Quenched in air |
| $NaCo_{0.8}Fe_{0.2}O_2$ | 850 | 3 | Quenched in air and put under argon |
| $NaCo_{0.9}Fe_{0.1}O_2$ | 950 | 22 | As mentioned above |
| $NaCoO_2$ | 550 | 10 | As mentioned above |

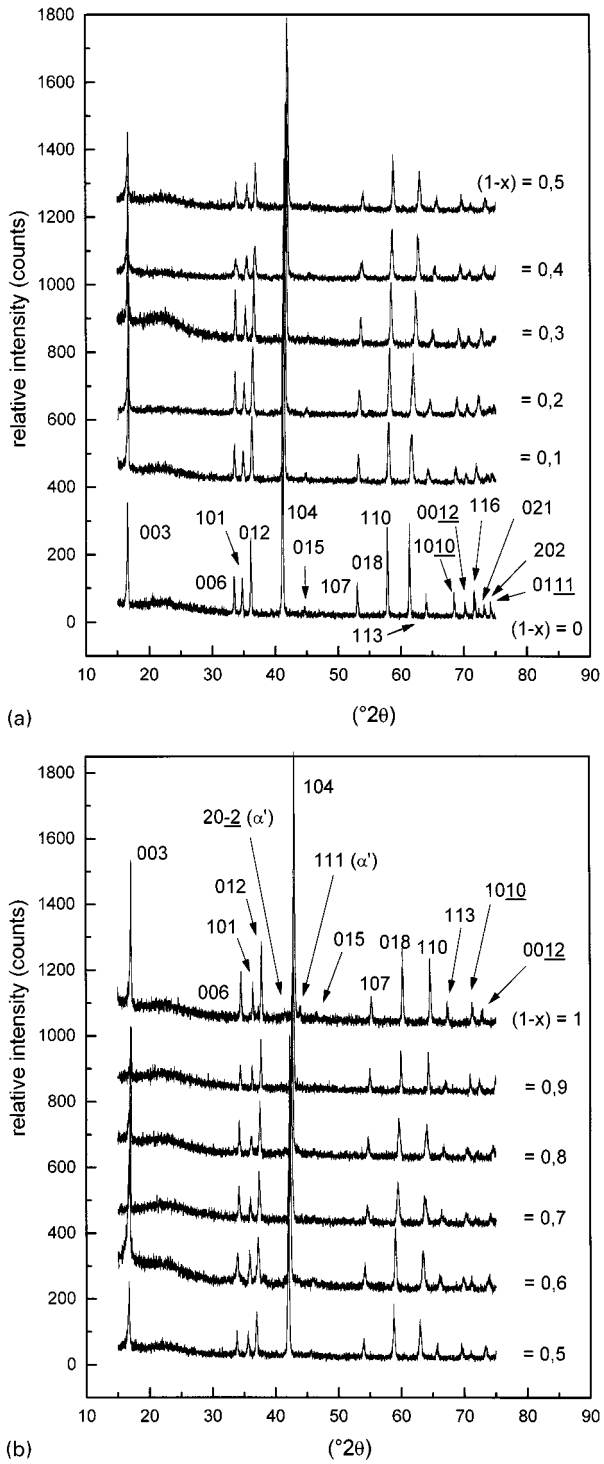


**FIG. 1.** XRD diagrams for some compounds of the system $NaCo_{1-x}Fe_xO_2$. The Miller indices are given for each Bragg peak with reference to the hexagonal setting of the rhombohedral $\alpha$-$NaFeO_2$ cell (space group $R\bar{3}m$). The spectra are shifted along the $y$ axis for clarity.

$\alpha$-$NaFeO_2$ structure type ($R\bar{3}m$). With increasing cobalt content the $a$- and $c$-lattice constants become smaller and the diffraction angles $^\circ 2\theta$ are shifted to higher values because of the lower radius of $Co^{3+}$ ($t_{2g}^6$, ls, $r = 0.545$ Å (39)) compared to that of $Fe^{3+}$ ($t_{2g}^3\, e_g^2$, hs, $r = 0.645$ Å).

The composition of the reaction products, which was determined by atomic absorption spectroscopy (Table 2) matches fairly well the intended stoichiometry and the possible formation of oxygen-deficient phases $NaCo_{1-x}Fe_xO_{2-\delta}$ (reported in (38) for $NaCoO_2$) did not take place. However, $NaCoO_2$ was not obtained single phase; two additional peaks at $2\theta = 41.52^\circ$ and $2\theta = 43.93^\circ$ could be attributed to monoclinic $\alpha$-$Na_{0.75}CoO_2$, whereas all other peaks can be indexed rhombohedrically to $\alpha$-$NaCoO_2$. The obtained sodium content of 0.94 to 1.02 Na per formula unit points out that, despite the 5% excess used, a partial volatilization of the sodium peroxide at the reaction temperatures occurred.

The dependency of the $a$- and $c$-lattice constants from $x$ is shown in Fig. 2. A nearly Vegard-like behavior can be observed for both lattice constants, which clearly shows that over the whole composition range a solid solution with $\alpha$-$NaFeO_2$-structure is formed where iron ions are continuously replaced by cobalt ions in the iron layer.

From the employed reaction temperatures and firing periods it can be concluded that small cobalt contents lower the formation rate of the layered structure compounds so that higher reaction temperatures and times are necessary. This behavior is observed until a cobalt content of $(1 - x) = 0.6$ is reached. At $(1 - x) = 0.7, 0.8$, the formation rate of the layered structure compound is drastically increased but the latter is thermodynamically stable only at the applied reaction temperature and it is necessary to quench the reaction mixture in order to avoid the formation of side products on cooling. For $(1 - x) = 0.9$ the compound is thermodynamically stable in a small window around 950°C. The pure layered structure cobalt phase $\alpha$-$NaCoO_2$ is not accessible at such temperatures. Even at the moderate temperatures applied it is only metastable but can be obtained kinetically favored over the monoclinic side product.

### 3.2. The System $LiCo_{1-x}Fe_xO_2$

#### *3.2.1. Analytical Results*

All samples showed a slightly lower lithium content than expected, whereas sodium could still be found in small quantities of approx. 5–6% (Table 3). These results may be explained either by sodium ions remaining in the lithium layers because of incomplete ion exchange or by a small percentage of a second sodium-containing phase. The average oxidation numbers determined (Table 4) show that the transition metal ions are present in the 3 + oxidation state. The reaction between $NaCo_{1-x}Fe_xO_2$ and a molten eutectic mixture of LiCl and $LiNO_3$ thus leads to nearly complete ion exchange.

**TABLE 2**
**AAS-Analytical Results of the $NaCo_{1-x}Fe_xO_2$ Compounds**

| Stoichiometry calculated | Sodium (%) | | Iron (%) | | Cobalt (%) | | Stoichiometry found |
|---|---|---|---|---|---|---|---|
| | Th. | Exp. | Th. | Exp. | Th. | Exp. | |
| $NaFeO_2$ | 20.7 | 20.3 | 50.4 | 49.3 | – | | $Na_{1.00}Fe_{1.00}O_2$ |
| $NaCo_{0.1}Fe_{0.9}O_2$ | 20.7 | 19.2 | 45.2 | 45.3 | 5.3 | 4.8 | $Na_{0.95}Co_{0.09}Fe_{0.92}O_2$ |
| $NaCo_{0.2}Fe_{0.8}O_2$ | 20.6 | 19.8 | 40.1 | 39.3 | 10.6 | 10.8 | $Na_{0.98}Co_{0.21}Fe_{0.8}O_2$ |
| $NaCo_{0.3}Fe_{0.7}O_2$ | 20.6 | 19.6 | 35.0 | 35.3 | 15.8 | 15.1 | $Na_{0.97}Co_{0.30}Fe_{0.71}O_2$ |
| $NaCo_{0.4}Fe_{0.6}O_2$ | 20.5 | 19.9 | 29.9 | 28.9 | 21.0 | 20.1 | $Na_{1.02}Co_{0.39}Fe_{0.60}O_2$ |
| $NaCo_{0.5}Fe_{0.5}O_2$ | 20.5 | 19.2 | 24.8 | 26.1 | 26.2 | 26.4 | $Na_{0.94}Co_{0.50}Fe_{0.52}O_2$ |
| $NaCo_{0.6}Fe_{0.4}O_2$ | 20.4 | 19.8 | 19.8 | 18.7 | 31.4 | 30.3 | $Na_{1.02}Co_{0.59}Fe_{0.39}O_2$ |
| $NaCo_{0.7}Fe_{0.3}O_2$ | 20.3 | 19.3 | 14.8 | 15.8 | 36.5 | 35.2 | $Na_{0.96}Co_{0.69}Fe_{0.32}O_2$ |
| $NaCo_{0.8}Fe_{0.2}O_2$ | 20.3 | 18.5 | 9.9 | 9.9 | 41.6 | 39.6 | $Na_{1.00}Co_{0.78}Fe_{0.22}O_2$ |
| $NaCo_{0.9}Fe_{0.1}O_2$ | 20.2 | 19.5 | 4.9 | 5.8 | 46.7 | 44.9 | $Na_{0.99}Co_{0.88}Fe_{0.12}O_2$ |
| $NaCoO_2$ | 20.2 | 20.2 | — | | 51.7 | 49.4 | $Na_{1.02}Co_{0.99}O_2$ |

### 3.2.2. *X-ray Diffraction*

The products are obtained single phase according to the XRD results shown in Fig. 3. Only in the case of $LiCo_{0.2}Fe_{0.8}O_2$ is a second phase visible (two additional reflections at $2\theta = 18.95°$ and $2\theta = 45.25°$), which has been identified as $LiCoO_2$. In the case of $LiFeO_2$ the crystal structure cannot be deduced from the diffraction pattern alone. The observed pattern points to the presence of a face-centered unit cell ($Fm\bar{3}m$). On the other hand, the formation of a layered structure of $\alpha$-$NaFeO_2$ type with $a$ $c/a$ value near 4.90 (value for an ideal cubic closed-packed array) cannot be excluded. In the latter case the observed extinctions are compatible with the trigonal space group $R\bar{3}m$ of $\alpha$-$NaFeO_2$ type. Figure 4 shows a comparison of the diffraction patterns obtained from a compressed sample pellet and from powder, an increase in the 00l reflections is detected for the pelletized sample. The pronounced two-dimensionality of the $\alpha$-$NaFeO_2$ type offers an opportunity to recognize the layered nature of such materials. Under applied pressure a preferred orientation is developed with the $c$-axis lying normal to the surface plane. This effect is easily detectable by a strong increase of the 00l reflections in the XRD of pressed pellets, whereas this behavior is absent in cubic materials (16). From the observed increase of the 00l reflections the presence of a layered material of $\alpha$-$NaFeO_2$ type can thus be deduced.

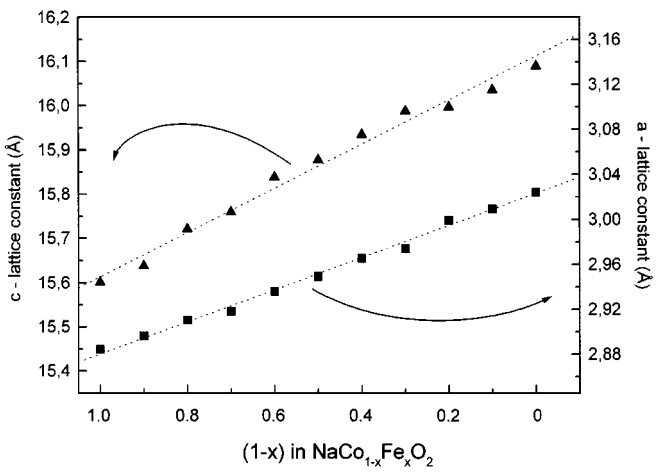


**FIG. 2.** Hexagonal lattice constants for the series $NaCo_{1-x}Fe_xO_2$ as a function of the cobalt content $(1 - x)$.

The $LiCo_{1-x}Fe_xO_2$ compounds crystallize in $\alpha$-$NaFeO_2$ type too and increasing cobalt content results in decreasing lattice constants (Fig. 5) as in the case of the sodium system. Moreover, as a consequence of the increasing $c/a$ ratio, a clear separation of the diffraction patterns (006)/(012) and (108)/(110) becomes visible, starting at $(1 - x) = 0.3$.

The $a$ constant shows Vegard-like behavior, whereas for the $c$ value and consequently for the $c/a$ ratio strong deviations from this behavior are observed. In the system $NaCo_{1-x}Fe_xO_2$ the difference in the ionic radii of $Na^+$ (1.02 Å) and $Co^{3+}/Fe^{3+}$ (0.55/0.65 Å) (39) is large; thus, ordering of $Na^+$ in 3$a$ and $Me^{3+}$ in 3$b$ is expected. Therefore the mean radius of the $d$-block elements is responsible for the distance of the slabs, whereas the distance of the sodium layers remains unchanged. Hence, the expected linear variation of the lattice constants is observed.

Almost perfect cation-ordering is known for $LiCoO_2$. The increase in the c-lattice constant for low iron content is higher than expected for a simple substitution of $Co^{3+}$ for $Fe^{3+}$.

Assuming a partial disorder of $Fe^{3+}$ in the 3$a$ sites implies a partial occupation of the 3$b$ positions by lithium (no iron excess has been found; therefore iron occupation of 3$a$ is supposed to be accompanied by lithium occupation of 3$b$ sites). The higher ionic radius of $Li^+$ in comparison to $Fe^{3+}$

**TABLE 3**
**AAS-Analytical Results of the $LiCo_{1-x}Fe_xO_2$ Compounds**

| Stoichiometry calculated | Lithium (%) | | Sodium (%) | | Iron (%) | | Cobalt (%) | | Stoichiometry found |
|---|---|---|---|---|---|---|---|---|---|
| | Th. | Exp. | Th. | Exp. | Th. | Exp. | Th. | Exp. | |
| $LiFeO_2$ | 7.3 | 7.2 | — | 1.8 | 58.9 | 59.7 | — | | $Li_{0.97}Na_{0.07}Fe_{1.00}O_2$ |
| $LiCo_{0.1}Fe_{0.9}O_2$ | 7.3 | 7.3 | — | 1.4 | 52.9 | 53.6 | 6.2 | 5.1 | $Li_{0.99}Na_{0.06}Co_{0.08}Fe_{0.90}O_2$ |
| $LiCo_{0.2}Fe_{0.8}O_2$ | 7.3 | 7.1 | — | 2.0 | 46.8 | 44.5 | 12.4 | 11.8 | $Li_{0.96}Na_{0.09}Co_{0.19}Fe_{0.79}O_2$ |
| $LiCo_{0.3}Fe_{0.7}O_2$ | 7.3 | 7.5 | — | 1.4 | 40.8 | 39.2 | 18.5 | 16.8 | $Li_{1.03}Na_{0.06}Co_{0.27}Fe_{0.67}O_2$ |
| $LiCo_{0.4}Fe_{0.6}O_2$ | 7.2 | 7.2 | — | 2.0 | 34.9 | 34.3 | 24.6 | 24.0 | $Li_{0.94}Na_{0.08}Co_{0.39}Fe_{0.60}O_2$ |
| $LiCo_{0.5}Fe_{0.5}O_2$ | 7.2 | 7.2 | — | 2.0 | 29.0 | 27.8 | 30.6 | 28.6 | $Li_{1.02}Na_{0.08}Co_{0.48}Fe_{0.49}O_2$ |
| $LiCo_{0.6}Fe_{0.4}O_2$ | 7.2 | 7.2 | — | 1.0 | 23.1 | 22.5 | 36.6 | 35.8 | $Li_{0.94}Na_{0.04}Co_{0.61}Fe_{0.40}O_2$ |
| $LiCo_{0.7}Fe_{0.3}O_2$ | 7.2 | 7.2 | — | 1.5 | 17.3 | 16.9 | 42.6 | 41.8 | $Li_{1.04}Na_{0.06}Co_{0.69}Fe_{0.30}O_2$ |
| $LiCo_{0.8}Fe_{0.2}O_2$ | 7.1 | 7.0 | — | 0.6 | 11.5 | 11.6 | 48.5 | 47.7 | $Li_{0.98}Na_{0.03}Co_{0.79}Fe_{0.21}O_2$ |
| $LiCo_{0.9}Fe_{0.1}O_2$ | 7.1 | 7.0 | — | 1.2 | 5.7 | 6.5 | 54.4 | 52.3 | $Li_{1.00}Na_{0.05}Co_{0.88}Fe_{0.11}O_2$ |
| IA–$LiCoO_2$ | 7.1 | 7.1 | — | 0.9 | — | | 60.2 | 58.7 | $Li_{1.03}Na_{0.04}Co_{0.97}O_2$ |
| HT–$LiCoO_2$ | 7.1 | 7.1 | — | 0 | — | | 60.2 | 60.8 | $Li_{1.00}Co_{1.00}O_2$ |

and $Co^{3+}$ causes an inflation of the $M^{3+}$ layers and thus an enlarged $c$ value as a consequence of increasing disorder.

Supposing that from an iron content of $x = 0.4$ on the disorder does not change further, a less steep linear increase can be expected until $LiFeO_2$ is reached, for which only cobalt substitution for iron in 3*b* is responsible. Hence, the XRD results indicate a partial disorder of $Fe^{3+}$ in 3*a* sites which has reached the value also present in $LiFeO_2$ already at $x \sim 0.4$.

HT-$LiCoO_2$ has been obtained as single phase product and XRD shows a diffraction pattern comparable to IE-$LiCoO_2$ with the same lattice constants. IE-$LiCoO_2$ shows broader reflections implying smaller crystallite size compared to HT-$LiCoO_2$, which is due to the much lower synthesis temperature of 550°C/260°C.

*Intensity ratio considerations.* The two intensity ratios $R_{003} = I_{003}/I_{104}$ and $R_{012} = (I_{006} + I_{012})/I_{101}$ have been introduced (40–42) as a measure of cation ordering in the system $Li_xNi_{2-x}O_2$. A more regular separation in cation layers for higher values of $R_{003}$ and lower values of $R_{012}$, respectively, can be explained by regarding the transition

**TABLE 4**
**Average Oxidation Number of the $LiCo_{1-x}Fe_xO_2$ Phases**

| Stoichiometry | Determined oxidation number |
|---|---|
| $LiFeO_2$ | Fe (+ 3.02) |
| $LiCo_{0.1}Fe_{0.9}O_2$ | Co (+ 3.22) |
| $LiCo_{0.2}Fe_{0.8}O_2$ | Co (+ 3.04) |
| $LiCo_{0.3}Fe_{0.7}O_2$ | Co (+ 3.04) |
| $LiCo_{0.4}Fe_{0.6}O_2$ | Co (+ 2.99) |
| $LiCo_{0.5}Fe_{0.5}O_2$ | Co (+ 3.02) |
| $LiCo_{0.6}Fe_{0.4}O_2$ | Co (+ 3.01) |
| $LiCo_{0.7}Fe_{0.3}O_2$ | Co (+ 3.00) |
| $LiCo_{0.8}Fe_{0.2}O_2$ | Co (+ 3.00) |
| $LiCo_{0.9}Fe_{0.1}O_2$ | Co (+ 3.03) |
| IA–$LiCoO_2$ | Co (+ 2.98) |
| HT–$LiCoO_2$ | Co (+ 2.98) |

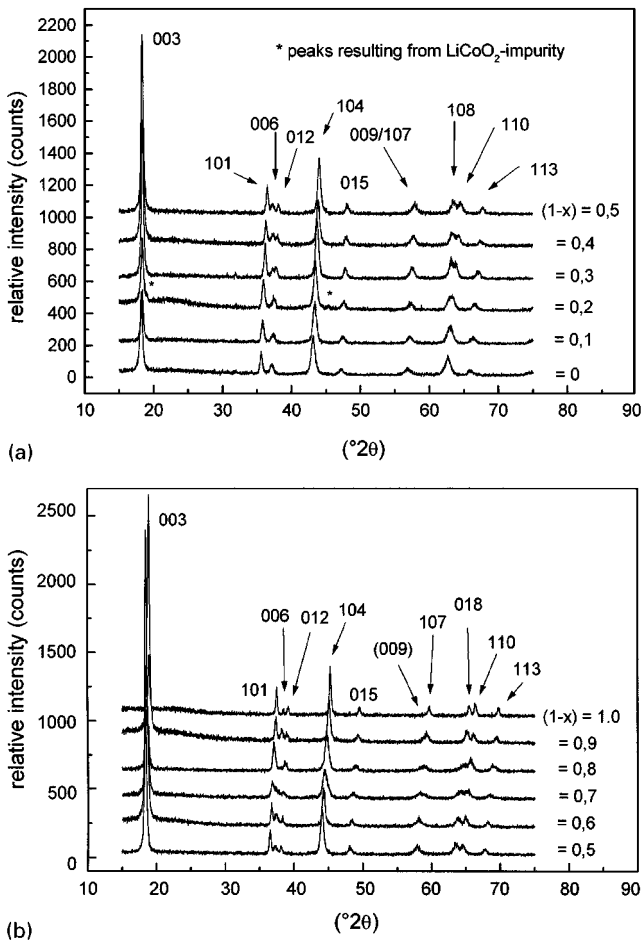


**FIG. 3.** XRD diagramms for several compounds of the system $LiCo_{1-x}Fe_xO_2$. The spectra are shifted along the y axis for clarity. (* Peaks resulting from $LiCoO_2$ impurity).

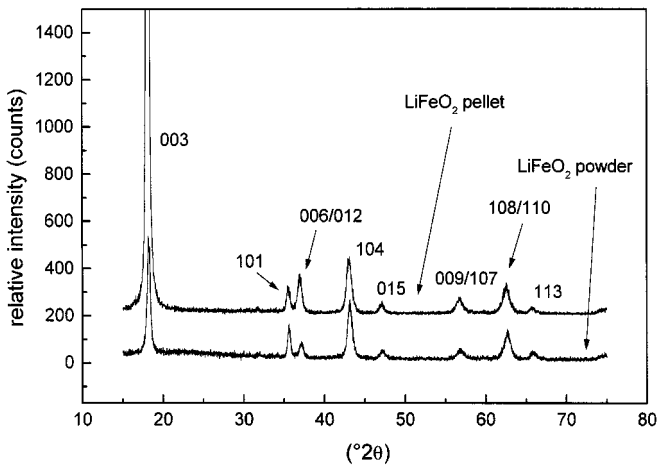


**FIG. 4.** Comparison of the XRD for $LiFeO_2$ in form of powder and pressed pellet. The spectra are shifted along the *y* axis.

from $LiNiO_2$, crystallizing in α-$NaFeO_2$-structure ($R\bar{3}m$) with layered cation ordering, to NiO, crystallizing in the cubic rock salt structure ($Fm\bar{3}m$) with no two-dimensional cation ordering (43). In the course of this transition the (003)-reflection of the space group $R\bar{3}m$ turns into the (111)-reflection of the space group $Fm\bar{3}m$ and therefore loses in intensity, raising the value of $R_{003}$. In the same direction the intensity of the (101)-reflection decreases compared to the intensity of the sum of the (006)- and (012)-reflections; hence for a more pronounced 2D cation ordering lower values of $R_{012}$ are obtained. Because of the preferred orientation that may occur at the examined layered oxides, resulting in higher intensities of (00l)-reflections, a simple comparison of the mentioned ratio values is not possible. Therefore the intensity ratio $R_{101} = I_{101}/I_{104}$ is regarded, employing no (00l)-reflections. As $I_{101}$ increases for the transition of a cubic into a rhombohedral lattice, whereas $I_{104}$ remains about the same, a higher value of $R_{101}$ can be expected for a higher degree of cation ordering.

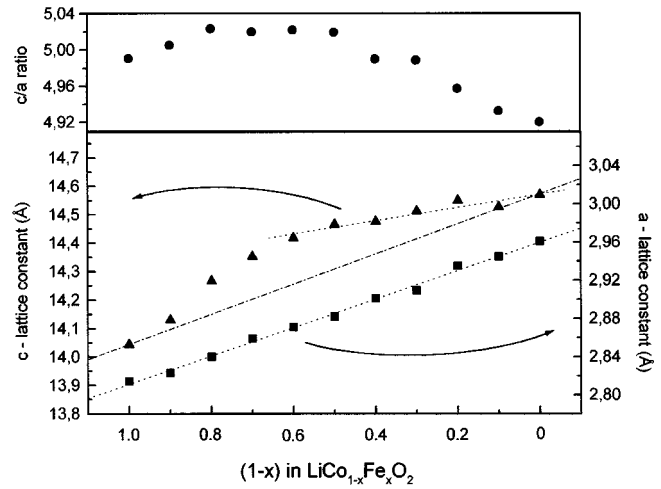


**FIG. 5.** Hexagonal lattice constants and *c*/*a* ratio for $LiCo_{1-x}Fe_xO_2$ as a function of the composition $(1 - x)$. Squares denote the *a* constant, triangles the *c* constant. The top part shows the *c*/*a* ratio. The dashed line denotes the course of the lattice constant for a hypothetic Vegard-like behavior.

*Structure refinements.* Structure refinements by the Rietveld method were performed using FULLPROF 90 for both $LiCoO_2$ compounds as well as for $LiFeO_2$ and $LiCo_{0.6}Fe_{0.4}O_2$. Scan steps and scan times per step were chosen as follows: HT-$LiCoO_2$, 0.01°, 10 s; IE-$LiCoO_2$, 0.02°, 20 s; $LiCo_{0.6}Fe_{0.4}O_2$, 0.01°, 20 s; $LiFeO_2$, 0.02°, 30 s. It has been assumed that the compounds are crystallizing single phase in α-$NaFeO_2$ type with $Li^+$ in 3*a*- (000),

**TABLE 5**
**Profile Refinement results on $LiCo_{1-x}Fe_xO_2$ Obtained with FULLPROF 90**

| Atom | Position | Occupation | *x* | *y* | *z* | |
|---|---|---|---|---|---|---|
| | | | | | | *HT-LiCoO₂* |
| Li | 3*a* | 1.002(2) | 0 | 0 | 0 | $a = 2.8146(9)$ Å; $c = 14.0537(20)$ Å |
| Li | 3*b* | − 0.002(2) | 0 | 0 | 0.5 | $B = 0.50$ Å² |
| Co | 3*a* | − 0.002(2) | 0 | 0 | 0 | $R_p = 9.87$; $R_{wp} = 12.6$ |
| Co | 3*b* | 1.002(2) | 0 | 0 | 0.5 | $R_{Bragg} = 5.84$ |
| O | 6*c* | 1.000 | 0 | 0 | 0.2392(7) | $R_f = 5.57$ |
| | | | | | | *IA-LiCoO₂* |
| Li | 3*a* | 1.007(3) | 0 | 0 | 0 | $a = 2.8131(17)$ Å; $c = 14.0534(42)$ Å |
| Li | 3*b* | − 0.007(3) | 0 | 0 | 0.5 | $B = 0.444$ Å² |
| Co | 3*a* | − 0.007(3) | 0 | 0 | 0 | $R_p = 6.51$; $R_{wp} = 8.49$ |
| Co | 3*b* | 1.007(3) | 0 | 0 | 0.5 | $R_{Bragg} = 3.45$ |
| O | 6*c* | 1.000 | 0 | 0 | 0.2390(5) | $R_f = 4.29$ |
| | | | | | | *$LiCo_{0.6}Fe_{0.4}O_2$* |
| Li | 3*a* | 0.955(3) | 0 | 0 | 0 | $a = 2.8568(35)$ Å; $c = 14.3551(89)$ Å |
| Li | 3*b* | 0.045(3) | 0 | 0 | 0.5 | $B = 0.555$ Å² |
| Co | 3*a* | 0.000(3) | 0 | 0 | 0 | $R_p = 7.27$; $R_{wp} = 9.46$ |
| Co | 3*b* | 0.600(3) | 0 | 0 | 0.5 | $R_{Bragg} = 6.23$ |
| Fe | 3*a* | 0.045 | 0 | 0 | 0 | $R_f = 7.38$ |
| Fe | 3*b* | 0.355 | 0 | 0 | 0.5 | |
| O | 6*c* | 1.000 | 0 | 0 | 0.2391(5) | |
| | | | | | | *LiFeO₂* |
| Li | 3*a* | 0.954(2) | 0 | 0 | 0 | $a = 2.9497(31)$ Å; $c = 14.5327(76)$ Å |
| Li | 3*b* | 0.046(2) | 0 | 0 | 0.5 | $B = 0.645$ Å² |
| Fe | 3*a* | 0.046(2) | 0 | 0 | 0 | $R_p = 9.22$; $R_{wp} = 12.8$ |
| Fe | 3*b* | 0.954(2) | 0 | 0 | 0.5 | $R_{Bragg} = 3.46$ |
| O | 6*c* | 1.000 | 0 | 0 | 0.2433(4) | $R_f = 3.50$ |

$Co^{3+}/Fe^{3+}$ in 3*b*- ($00\frac{1}{2}$), and $O^{2-}$ in 6*c*-positions ($00\frac{1}{4}$). Occupation of the oxide sites is believed to be regular and the reflections to be of pseudo-Voigt-profile. To account for the preferred orientation possible the parameters describing the further have been varied too. Only such variations were allowed that were consistent with the following formula: $(Li_{1-u}Me_u)_{3a}(Li_uMe_{1-u})_{3b}(O_2)_{6c}$. The sodium content was not taken into account for Rietveld refinement because of the omnipresence of $Na^+$ leading to eventual experimental mistakes in the order of magnitude of the measured values and because it is not clear if the sodium is present in the layered structure material or in a second phase, in a percentage too small to be detected by XRD technique.

The results of the refinement are shown in Table 5 and the observed and calculated diffraction patterns in Fig. 6. They indicate that the assumption of $\alpha$-$NaFeO_2$ type for the series $LiCo_{1-x}Fe_xO_2$ is correct. In the case of the $LiCoO_2$ samples a small negative value for the disorder in 3*a* position was obtained ($-0.2$ and $-0.7\%$ for HT- and IE-$LiCoO_2$, respectively).

Reimers *et al.* (44) explained this effect of a negative occupation ($-1.7\%$ for $LiCoO_2$) with phase separation, i.e., besides $LiCoO_2$ without disorder the sample contains small amounts of CoO. For the present materials the effects are below 1%, so that these considerations could not be proved by XRD and AAS results. In both $LiCoO_2$ no cobalt disorder can be observed and IE-$LiCoO_2$, in contrast to the LT-$LiCoO_2$ examined by Gummow *et al.* (45), crystallizes in the same structure as HT-$LiCoO_2$.

$LiFeO_2$ shows a cationic disorder of 4.5%. For $LiCo_{0.6}Fe_{0.4}O_2$ 4.5% was calculated too, a fact that agrees with the above-mentioned appreciable disorder already present for low iron contents. The obtained cationic disorder for $LiFeO_2$ is in agreement with published values (5–8% (9), 5% (46), 2% (13)).

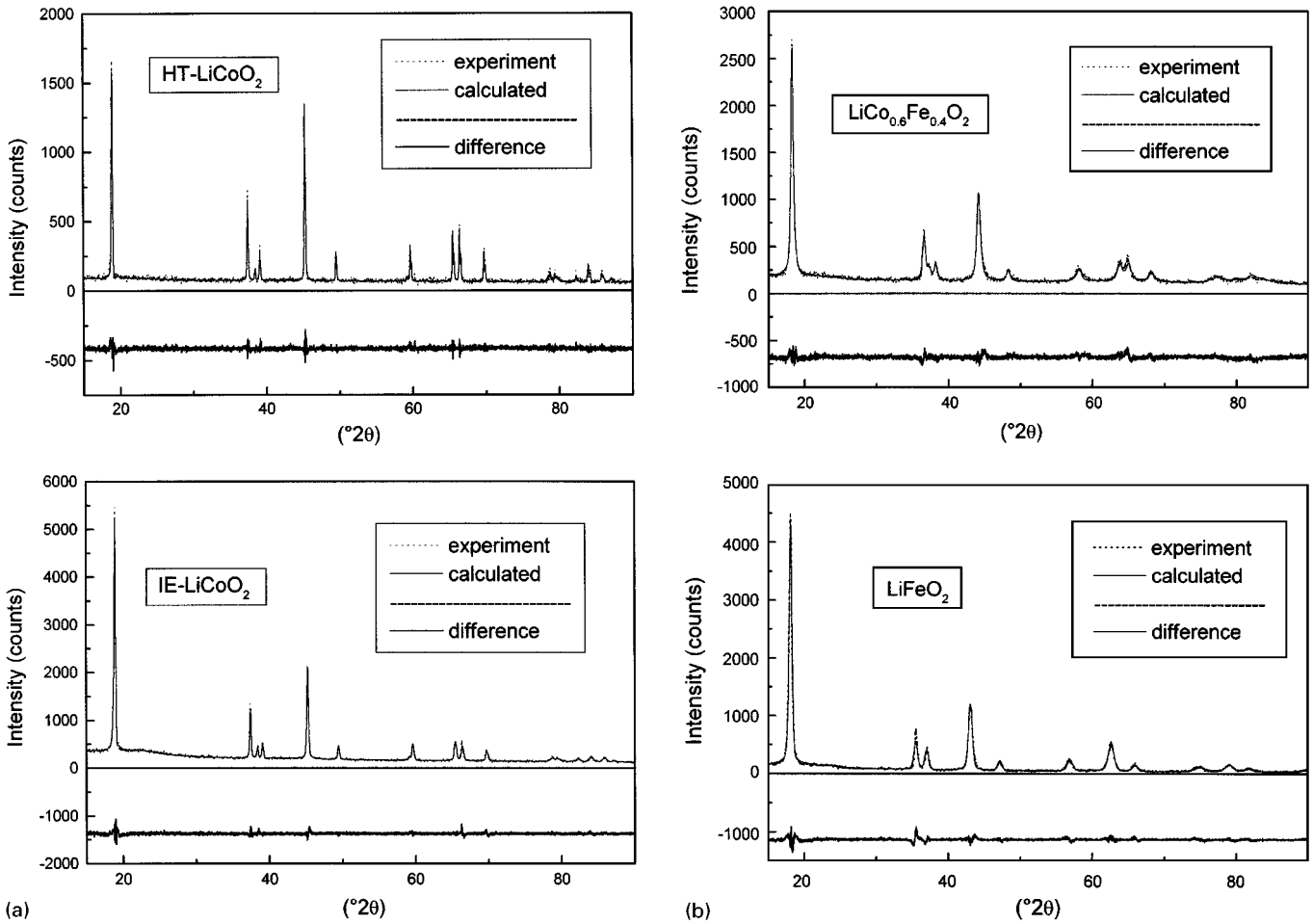


**FIG. 6.** Calculated and observed X-ray diffraction profiles for the series $LiCo_{1-x}Fe_xO_2$.

**TABLE 6**
**Intensity Ratios $R_{003}$, $R_{012}$, and $R_{101}$ for $LiCoO_2$, $LiFeO_2$, and $LiCo_{0.6}Fe_{0.4}O_2$**

| Intensity ratio | HT-$LiCoO_2$ | IE-$LiCoO_2$ | $LiCo_{0.6}Fe_{0.4}O_2$ | $LiFeO_2$ |
|---|---|---|---|---|
| $R_{003}$ (observed) | 1.23 | 2.45 | 1.70 | 2.61 |
| $R_{003}$ (calculated) | 1.18 | 2.38 | 1.73 | 2.67 |
| $R_{012}$ (observed) | 0.42 | 0.54 | 0.64 | 0.71 |
| $R_{012}$ (calculated) | 0.46 | 0.54 | 0.62 | 0.77 |
| $R_{101}$ (observed) | 0.48 | 0.48 | 0.38 | 0.36 |
| $R_{101}$ (calculated) | 0.46 | 0.48 | 0.41 | 0.37 |

*Note*. The calculated values have been obtained from the Rietveld profile refinement.

As the system $Li_xNi_{2-x}O_2$ differs from the system $(Li_{1-u}Me_u)_{3a}(Li_uMe_{1-u})_{3b}(O_2)_{6c}$, the considerations on the intensity ratios of the former cannot be quantitatively applied to our system, but the general trend remains the same, as for $u = 0.5$ a disordered cubic lattice would be obtained. Nevertheless, the obtained $R_{101}$ values (shown in Table 6) have been regarded only qualitatively. It can be seen, that for the two $LiCoO_2$ samples the values obtained are about the same and that $LiCo_{0.6}Fe_{0.4}O_2$ is more similar to $LiFeO_2$ than to $LiCoO_2$, despite the fact that it contains more cobalt than iron. From Table 6 it can also be seen, that $R_{003}$ and $R_{012}$ show no clear trend. This may be due to an appreciable amount of preferred orientation of the crystal plates.

Reimers (47) obtained up to 9% of iron occupation in 3*a* for the system $LiNi_{1-x}Fe_xO_2$ ($0 \le x \le 0.4$), prepared by solid-state reaction. Kanno (9) *et al.* did not publish refinement results of their $LiNi_{1-x}Fe_xO_2$ obtained by ion exchange from $NaNi_{1-x}Fe_xO_2$, but nevertheless the degree of cation ordering in the system $LiCo_{1-x}Fe_xO_2$ seems to be somewhat higher than in the system $LiNi_{1-x}Fe_xO_2$, which is not surprising taking into consideration the higher degree of cation ordering in the parent phase $LiCoO_2$ compared to $LiNiO_2$.

By this way no information can be obtained about whether the distribution of the transition metal ions is random or if clustering occurs. High magnetic field measurements and the behavior of the magnetization vs temperature curves performed on the compounds point to random ion distribution in the transition metal layer (32). For low iron contents ($x \le 0.1$), however, nonrandom distribution of $Fe^{3+}$ and $Co^{3+}$ ions in the octahedral sites has been suggested by Alcántara *et al.* (48). Final proof of the supposed structure model cannot be given by XRD-Rietveld-technique alone. It is, however, strongly supported by the afore-mentioned magnetic data, and measuring time at ILL in Grenoble has been accorded to us in order to proof structural and an eventual magnetic ordering by neutron diffraction.

### *3.2.3. Infrared Spectroscopic Examination of $LiCo_{1-x}Fe_xO_2$*

According to the theoretical group analysis the number of IR-active modes for $LiCoO_2$ is four (49, 50). These bands can be separated into vibrations of the cobalt layers (situated between 400 and 700 $cm^{-1}$) and the lithium layers (200–300 $cm^{-1}$). Alcántara *et al.* (51) found in $LiCoO_2$ four bands situated at 535, 554, 598, and 646 $cm^{-1}$. As is evidenced by Fig. 7 and Table 7 three bands can be resolved in the IR spectrum of IE-$LiCoO_2$, named $v_1$–$v_3$, the band at 554 $cm^{-1}$ is superimposed by the adjacent bands. The comparison of HT-$LiCoO_2$ with IE-$LiCoO_2$ shows a weaker separation but no displacement of the bands. For $Fe^{3+}$ substitution a displacement toward lower wavenumbers is detected. This behavior is due to the higher ionic radius of $Fe^{3+}$ ($O_h$ symmetry, high spin) compared to $Co^{3+}$ ($O_h$ symmetry, low spin), resulting in an increase in bond length

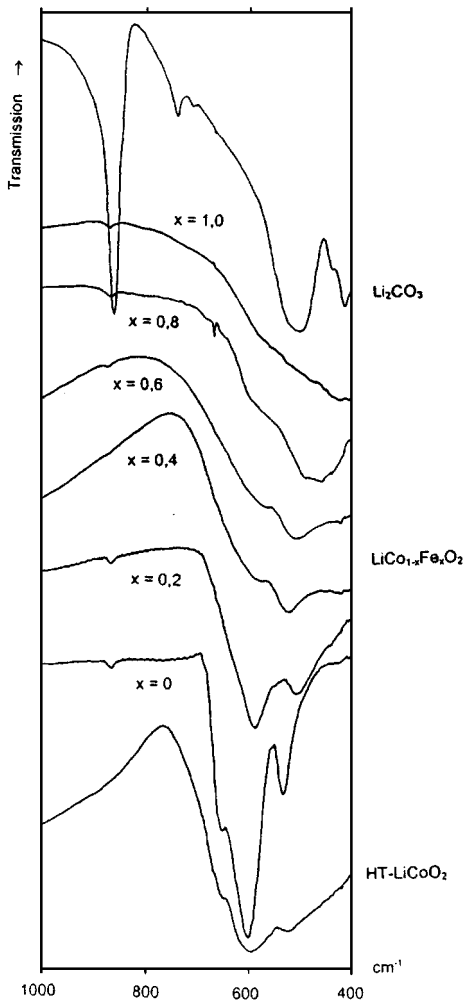


**FIG. 7.** Infrared spectra for several members of the series $LiCo_{1-x}Fe_xO_2$.

**TABLE 7**
**Experimentally Obtained Wavenumbers of the IR Bands for $LiCo_{1-x}Fe_xO_2$**

| Compound | $\nu_1$ ($cm^{-1}$) | $\nu_2$ ($cm^{-1}$) | $\nu_3$ ($cm^{-1}$) |
|---|---|---|---|
| $LiFeO_2$ | — | 425 | (570) |
| $LiCo_{0.2}Fe_{0.8}O_2$ | — | 465 | (575) |
| $LiCo_{0.4}Fe_{0.6}O_2$ | (425) | 510 | 565 |
| $LiCo_{0.6}Fe_{0.4}O_2$ | (425) | 525 | 580 |
| $LiCo_{0.8}Fe_{0.2}O_2$ | 505 | 590 | — |
| IA–$LiCoO_2$ | 535 | 605 | 640 |
| HT–$LiCoO_2$ | 530 | 600 | 645 |

and a decrease in bond strength. For $LiCo_{0.8}Fe_{0.2}O_2$ $\nu_3$ is not visible. The cobalt-rich samples show well distinguishable bands, whereas for $x = 0.8$ only two modes are visible: $\nu_2$ and $\nu_3$ as a weak shoulder of $\nu_2$. Small amounts of $Li_2CO_3$ in the products are evidenced at 860 $cm^{-1}$.

The comparison of HT-$LiCoO_2$ with IE-$LiCoO_2$ shows, besides the lower resolution of the former for which no explanation has been found, no band shift, in accordance with the same structure type found in the two samples. The observation that the sharpness of the bands decreases along with increasing iron content can be explained, according to Zhecheva *et al.* (27) with a lower degree of cation ordering. This results in a lower band separation and the reduction of the number of visible bands to two.

## 4. CONCLUSIONS

The sodium compounds $NaCo_{1-x}Fe_xO_2$ were prepared by solid-state reaction and characterized by X-ray diffraction. A solid solution of α-$NaFeO_2$ structure was obtained with mixing of $Fe^{3+}$ and $Co^{3+}$ in the crystallographic 3*b*-positions and without cation disorder between 3*a* and 3*b* sites. With increasing cobalt content the thermal stability of the compounds increases until $(1 - x) = 0.6$, whereas for $(1 - x) > 0.6$ the products can be obtained at the appropriate reaction temperature only as metastable products.

It has been demonstrated that the compounds of the $LiCo_{1-x}Fe_xO_2$ series (α-$NaFeO_2$ type structure, space group $R\bar{3}m$) can be obtained for $0 \leq x \leq 1$ using an ion exchange reaction from the corresponding sodium phases in a molten $LiCl/LiNO_3$ eutectic mixture. A low sodium content remains in the samples, possibly due to an incomplete ion exchange reaction or to the formation of an insoluble sodium containing secondary phase in quantities not detectable by XRD.

Layered rock salt structure has been proved for $LiFeO_2$ by the intensity increase of the 00l-reflections in XRD of a pressed sample and for increasing cobalt content by the splitting of (006)/(102)- and (018)/(110)-reflections.

X-ray diffraction shows that, in contrast to the $NaCo_{1-x}Fe_xO_2$ compounds, no simple substitution of cobalt for iron occurs and that the members of the $LiCo_{1-x}Fe_xO_2$ series show an increasing iron disorder which reaches a value of approx. 5% of iron ions on lithium sites for both $LiCo_{0.6}Fe_{0.4}O_2$ and $LiFeO_2$.

## ACKNOWLEDGMENTS

The authors thank Prof. Dr. S. Kemmler-Sack who supervised this work until her death and to whom the authors are much indebted. This publication had to be edited without her help. The authors are indebted as well to Mrs. E. Niquet and Mrs. A. Ehmann for their helpful assistance.

## REFERENCES

1. A. Lecerf, *Ann. Chim.* **7**(7–8), 520 (1962).
2. L. Croguennec, P. Deniard, and R. Brec, *J. Electrochem. Soc.* **144,** 3323 (1997).
3. R. J. Gummow and M. M. Thackeray, *J. Electrochem. Soc.* **141,** 1178 (1994).
4. P. G. Bruce, A. R. Armstrong, and H. Huang, *J. Power Sources* **68,** 19 (1997).
5. F. Capitaine, P. Gravereau, and C. Delmas, *Solid State Ionics* **89,** 197 (1996).
6. M. Tabuchi, K. Ado, H. Kobayashi, H. Kageyama, C. Masquelier, A. Kondo, and R. Kanno, *J. Electrochem. Soc.* **145,** L49 (1998).
7. R. Famery, P. Bassoul, and F. Queyroux, *J. Solid State Chem.* **57,** 178 (1985).
8. R. Famery, P. Bassoul, and F. Queyroux, *J. Solid State Chem.* **61,** 293 (1986).
9. R. Kanno, T. Shirane, Y. Inaba, and Y. Kawamoto, *J. Power Sources* **68,** 145 (1997).
10. R. Kanno, T. Shirane, Y. Kawamoto, Y. Takeda, M. Takano, M. Ohashi, and Y. Yamaguchi, *J. Electrochem. Soc.* **143,** 2435 (1996).
11. Y. Sakurai, H. Arai, S. Okada, and J. Yamaki, *J. Power Sources* **68,** 711 (1997).
12. J. B. Goodenough, W. A. England, K. Mizushima, and P. J. Wiseman, *Proc. Eur. Communities Meet. Adv. Batteries* 185 (1979).
13. K. Ado, M. Tabuchi, H. Kobayashi, H. Kageyama, and O. Nakamura, *J. Electrochem. Soc.* **144,** L177 (1997).
14. V. Nalbandyan and I. Sukaev, *Russ. J. Inorg. Chem.* (*Engl. Transl.*) **32,** 453 (1987).
15. S. Kikkawa, H. Ohkura, and M. Koizumi, *Mater. Chem. Phys.* **18,** 375 (1987).
16. B. Fuchs and S. Kemmler-Sack, *Solid State Ionics* **68,** 279 (1994).
17. T. Shirane, R. Kanno, Y. Kawamoto, Y. Takeda, M. Takano, T. Kamiyama, and F. Izumi, *Solid State Ionics* **79,** 277 (1995).
18. B. Fuchs, Ph.D. thesis, Universität Tübingen, 1993.
19. M. Holzapfel, Diplomarbeit, Universität Tübingen, 1998.
20. J. N. Reimers, E. Rossen, C. D. Jones, and J. R. Dahn, *Solid State Ionics* **61,** 335 (1993).
21. R. Kanno, H. Kubo, Y. Kawamoto, T. Kaniyama, F. Izumi, Y. Takeda, and M. Takano, *J. Solid State Chem.* **110,** 219 (1994).
22. A. Hirano, R. Kanno, Y. Kawamoto, Y. Takeda, K. Yamaura, M. Takano, K. Okyama, M. Ohashi, and Y. Yamaguchi, *Solid State Ionics* **78,** 123 (1995).
23. K. Mizushima, P. C. Jones, P. J. Wiseman, and J. B. Goodenough, *Mater. Res. Bull.* **15,** 783 (1980).
24. T. Ohzuku, A. Ueda, N. Nagayama, Y. Iwakoshi, and H. Komori, *Electrochim. Acta* **38,** 1159 (1993).

25. A. Rougier, I. Saadoune, P. Gravereau, P. Willmann, and C. Delmas, *Solid State Ionics* **90,** 83 (1996).
26. I. Saadoune and C. Delmas, *J. Solid State Chem.* **136,** 8 (1998).
27. E. Zhecheva and R. Stoyanova, *J. Solid State Chem.* **66,** 143 (1993).
28. Y. Fujita, K. Amine, J. Maruta, and H. Yasuda, *J. Power Sources* **68,** 126 (1997).
29. D. Caurant, N. Baffier, B. Garcia, and J. P. Pereira-Ramos, *Solid State Ionics* **91,** 45 (1996).
30. R. Alcántara, J. C. Jumas, P. Lavela, J. Olivier-Fourcade, C. Pérez-Vicente, and J. L. Tirado, *J. Power Sources* **81–82,** 547 (1999).
31. M. Tabuchi, K. Ado, H. Kobayashi, H. Sakaebe, H. Kageyama, C. Masquelier, M. Yonemura, A. Hirano, and R. Kanno, *J. Mater. Chem.* **9,** 199 (1999).
32. E. Chappel, M. Holzapfel, G. Chouteau, and A. Ott, *J. Solid State Chem.* **154,** 451 (2000).
33. M. Holzapfel, A. Ott, and R. Schreiner, *Electrchimica Acta*, in press.
34. Juan Rodriguez-Carvajal, Laboratoire Leon Brillouin (CEA-CNRS), France.
35. S. Miyazaki, S. Kikkawa, and M. Koizumi, *Synth. Met.* **6,** 211 (1983).
36. T. Ichida, T. Shinjo, Y. Bando, and T. Takada, *J. Phys. Soc. Jpn.* **29,** 95 (1970).
37. C. Fouassier, G. Matejka, J. M. Reau, and P. Hagenmuller, *J. Solid State Chem.* **6,** 532 (1973).
38. C. Delmas, C. Fouassier, and P. Hagenmuller, *Inorg. Synth.* **22,** 56 (1983).
39. R. D. Shannon, *Acta Crystallogr. A* **32,** 751 (1976).
40. R. V. Moshtev, P. Zlatilova, V. Manev, and A. Sato, *J. Power Sources* **54,** 329 (1995).
41. J. R. Dahn, U. von Sacken, and C. A. Michal, *Solid State Ionics* **44,** 87 (1990).
42. J. N. Reimers, J. R. Dahn, J. E. Greedan, C. V. Stager, G. Liu, J. Davidson, and U. von Sacken, *J. Solid State Chem.* **102,** 542 (1993).
43. W. Li, J. N. Reimers, and J. R. Dahn, *Phys. Rev. B* **46,** 3236 (1992).
44. J. N. Reimers and J. R. Dahn, *J. Electrochem. Soc.* **139,** 2091 (1992).
45. R. J. Gummow, D. C. Liles, and M. M. Thackeray, *Mater. Res. Bull.* **28,** 235 (1993).
46. V. Klein, Ph.D. thesis, Universität Tübingen, 1995.
47. J. N. Reimers, E. Rossen, C. D. Jones, and J. R. Dahn, *Solid State Ionics* **61,** 335 (1993).
48. R. Alcántara, P. Lavela, C. Pérez-Vicente, J. L. Tirado, J. Olivier-Fourcade, and J. C. Jumas, *Solid State Commun.* **115,** 1 (2000).
49. P. Tarte and J. Preudhomme, *Spectrochim. Acta* **26A,** 747 (1970).
50. R. K. Moore and W. B. White, *J. Am. Ceram. Soc.* **53,** 679 (1970).
51. R. Alcántara, P. Lavela, J. L. Tirado, R. Stoyanova, and E. Zhecheva, *J. Solid State Chem.* **134,** 265 (1997).